06

Broadband two-dimensional infrared spectroscopy with signal detection in visible range by nonlinear chirped-pulse upconversion

© E.A. Stepanov[1,2], G.D. Ivanov[1,2], A.N. Zhdanov[1], A.A. Voronin[1,2], A.S. Shvedov[1], I.V. Savitsky[1], A.A. Lanin[1,2], A.B. Fedotov[1,2,¶]

[1] Department of Physics, Moscow State University, Moscow, Russia
[2] Russian Quantum Center,
143025 Skolkovo, Russia

¶ e-mail: a.b.fedotov@physics.msu.ru

Received January 14, 2023
Revised June 10, 2023
Accepted August 04, 2023

The paper presents a technique for broadband two-dimensional infrared spectroscopy with signal detection in visible range by nonlinear chirped-pulse upconversion. This approach helps to avoid direct measurement of the mid-infrared signal that requires cryogenic technology, and instead uses low-cost high-sensitivity multichannel silicon linear arrays. This leads to a reduction by two orders of magnitude of the measurement time of a single two-dimensional spectrum, which makes it possible to observe the fast dynamics of complex molecular compounds. The use of a quasi-phase-cycling achieved by sub-cycle delay modulation suppresses scattering background by almost two orders of magnitude and increases the measurement speed twice compared to optical chopping. Numerical simulation using the density matrix formalism and analysis of its evolution based on the solution of the Bloch-Redfield equation effectively reproduces the features of the two-dimensional infrared spectrum of inorganic octacarbonyl dicobalt compound.

Keywords: Two-dimensional mid-infrared spectroscopy, ultrashort mid-infrared pulses, upconversion.

DOI: 10.61011/EOS.2023.08.57288.4531-23

The technique of two-dimensional infrared (IR) Fourier spectroscopy using ultrashort pulses of the mid-IR range is a modern method for studying fast dynamics in complex oscillatory systems, which is based on the nonlinear four-wave interaction of pulsed broadband IR radiation with the substance [1–7]. Femtosecond time resolution in combination with spectral selectivity and high spatial resolution make it possible to use two-dimensional IR spectroscopy in problems of characterizing rapidly interconverting substances and recording ultrafast processes in complex biological and chemical systems. Two-dimensional IR spectroscopy allows obtaining more information about the substance under study compared to one-dimensional techniques, identifying the relationship between interacting modes, observing the time evolution of vibrational frequencies, and determining the influence of the environment on the behavior of individual elements in complicated complexes and in solutions [1–7].

The 2D IR spectrum is measured using a sequence of three ultra-short mid-IR laser pulses with precisely controlled timing. The induced third-order nonlinear polarization in the medium can be written in the following form [1,5]

$$P^{(3)}(t) \propto \int_0^\infty d\tau_3 \int_0^\infty d\tau_2 \int_0^\infty d\tau_1 \, R(\tau_3, \tau_2, \tau_1) E(t-\tau_3) \times \\ \times E(t-\tau_3-\tau_2) E(t-\tau_3-\tau_2-\tau_1), \quad (1)$$

where $R(\tau_3, \tau_2, \tau_1)$ is third-order response function, which determination is the fundamental task of nonlinear spectroscopy. Two-dimensional spectroscopy allows measuring it with the greatest completeness, using a sequence of three ultra-short pulses that minimize the effect of convolution on the result. The pump field can be represented as a sequence of delta pulses:

$$E(t) = E_3\delta(t)e^{\pm i\omega t \mp ikr} + E_2\delta(t+t_2)e^{\pm i\omega t \mp ikr} + \\ + E_1\delta(t+t_2+t_1)e^{\pm i\omega t \mp ikr}, \quad (2)$$

where the first two pulses E_1 and E_2, lagging each other by a time t_1, are known as pump pulses, the third pulse E_3, delayed relative to the pumping by a waiting time t_2, is known as a sounding pulse or a probe pulse. The delta pulse approximation is valid when the characteristic times of the response function in the frequency range under study are much longer than the pulse duration. In the implemented configuration of two-dimensional IR Fourier spectroscopy, this condition is met because the pulse durations are tens of femtoseconds, while the characteristic times of evolution of the vibrational states of molecules are in the range from hundreds of femtoseconds to tens of picoseconds. Substituting the field represented as (2) into equation (1) taking into account a given sequence of pulses ($E_1 \to E_2 \to E_3$) and a certain direction of signal detection allows us to obtain a nonlinear signal proportional to the

third-order response function:

$$P^{(3)}(t) \propto E_1 E_2 E_3 \int_0^\infty d\tau_3 \int_0^\infty d\tau_2 \int_0^\infty d\tau_1 R(\tau_3, \tau_2, \tau_1) \times$$
$$\times \delta(t - \tau_3)\delta(t + t_2 - \tau_3 - \tau_2) \times$$
$$\times \delta(t + t_1 + t_2 - \tau_3 - \tau_2 - \tau_1) \propto R(t, t_2, t_1). \quad (3)$$

For detection, the nonlinear signal is mixed with the fourth, additional femtosecond pulse known as local oscillator, which is delayed by a time t_3 relative to the probe pulse. Thus, in the delta function approximation, the detected signal $S(t_3, t_2, t_1)$ at the output from the medium under study turns out to be directly proportional to the response function $R(t_3, t_2, t_1)$. The interpretation of the third-order response function in frequency representation is more understandable and informative, therefore, to visualize the two-dimensional spectrum, a two-dimensional Fourier transform is performed over t_1 and t_3 variables. The resulting two-dimensional spectrum contains information about the relationships between the excited and detected frequencies during the interaction of radiation with the substance, and varying the delay t_2 of the probe pulse allows obtaining „snapshots" to observe the dynamics of the state of molecules of the substance under study:

$$S(\omega_3, t_2, \omega_1) = \int_0^\infty \int_0^\infty S(t_3, t_2, t_1) e^{i\omega_1 t_1} e^{i\omega_3 t_3} dt_1 dt_3 =$$
$$= \int_0^\infty \int_0^\infty iR(t_3, t_2, t_1) e^{i\omega_1 t_1} e^{i\omega_3 t_3} dt_1 dt_3. \quad (4)$$

Experimental measurements in this study were carried out in one of the most common configuration for recording two-dimensional IR absorption spectrum with femtosecond time resolution [8], which is based on Michelson IR-interferometer, and pulses interact with the sample in the „pump-probe" geometry (Fig. 1). In such a geometry, the nonlinear response propagates strictly in the direction of the probe pulse, with the latter acting as a local oscillator ($t_3 = 0$). To measure one two-dimensional spectrum, it is necessary to scan the delay t_1 in a certain range at a fixed waiting time t_2 (Fig. 1, *b* shows the sequence of pulses incident to the sample under study). The Fourier transform is performed only for the variable t_1, and to obtain a spectrum along the ω_3 axis, the radiation of the nonlinear response is decomposed into a spectrum using a monochromator.

The mid-IR femtosecond pulse is generated in a laser system based on a kilohertz regenerative Ti:Sapphire amplifier of chirped pulses with subsequent frequency down-conversion in an optical parametric amplifier and a difference frequency generator based on a GaSe crystal [9,10]. The output pulse of the laser system with a duration of 60–100 fs is tunable in a wide range of wavelengths from 3 to 11 μm, reaching a maximum energy of 25 μJ (at a central wavelength of 3–5 μm). This pulse is split into two unequal replicas by a zinc selenide beam splitter with a small wedge (30'). A weak reflection with an energy of about 200 nJ is used as a probe beam, and a more powerful transmitted beam is introduced into the Michelson interferometer, where a pair of pump pulses with an adjustable delay t_1 is formed. This delay is determined with high accuracy by a quadrature detector from the interferogram formed in the same interferometer by a highly coherent He-Ne laser. The probe pulse passes through its own independent automated delay line (t_2), after which all three IR pulses are focused onto the sample by an off-axis parabolic mirror (PM1). After passing through the sample under study, the pump pulses are recorded by the IR MCT-diode D1, and the spectrum of the probe pulse is studied either directly in the IR range using a monochromator and a liquid nitrogen-cooled MCT-diode, or in the visible range after nonlinear optical frequency conversion in the process of generating the sum frequency with a reference pulse.

The theoretical maximum resolution of the „excitation spectrum" (along the horizontal axis of the two-dimensional IR spectrum) is determined by the scanning range of the delay t_1 between the arms of the pump interferometer. Thus, to obtain a resolution of the order of one inverse centimeter, it is necessary to scan the delay in the range of 30 ps. To restore the studied high-frequency components of the nonlinear spectrum, the distance between individual sampling moments should not exceed the radiation half-wavelength, and taking into account the loss of half of the laser „shots" for determining and subtracting the background illumination when using an optical chopper, it should not exceed quarter-wavelength. Together with the relatively low pulse repetition rate of the laser system (1 kHz), this imposes a limitation on the maximum delay scanning speed t_1 and results in the situation that at least 10 s are spent for one scan. Thus, in the implementation of a configuration with direct detection by a single-element IR detector, about 10 min are spent for the measuring a two-dimensional map with a resolution of 100×100 points with a spectral resolution of the order of one inverse centimeter.

The peak spectral power density of the absolute black body radiation at room temperature occurs at a wavelength of an order of 10 μm, therefore for the direct detection of radiation in the mid-IR range (3–10 μm), cooling of the detector to the temperature of liquid nitrogen is applied, which significantly increases the cost and complexity of the detector that can be made in both single-channel and multi-channel versions. To increase the speed of the system, we have implemented an alternative technique for spectral analysis of the IR probe pulse based on nonlinear optical frequency transfer of the signal under study to the visible region of the spectrum, i.e. up-conversion. This approach allows the use of more efficient and faster silicon CCD matrices and linear arrays to record the spectrum at once in the entire frequency range of interest, resulting in a two-order reduction in the time of collecting data of one two-dimensional spectrum. This opens up the possibility of studying the processes of fast chemical and biological

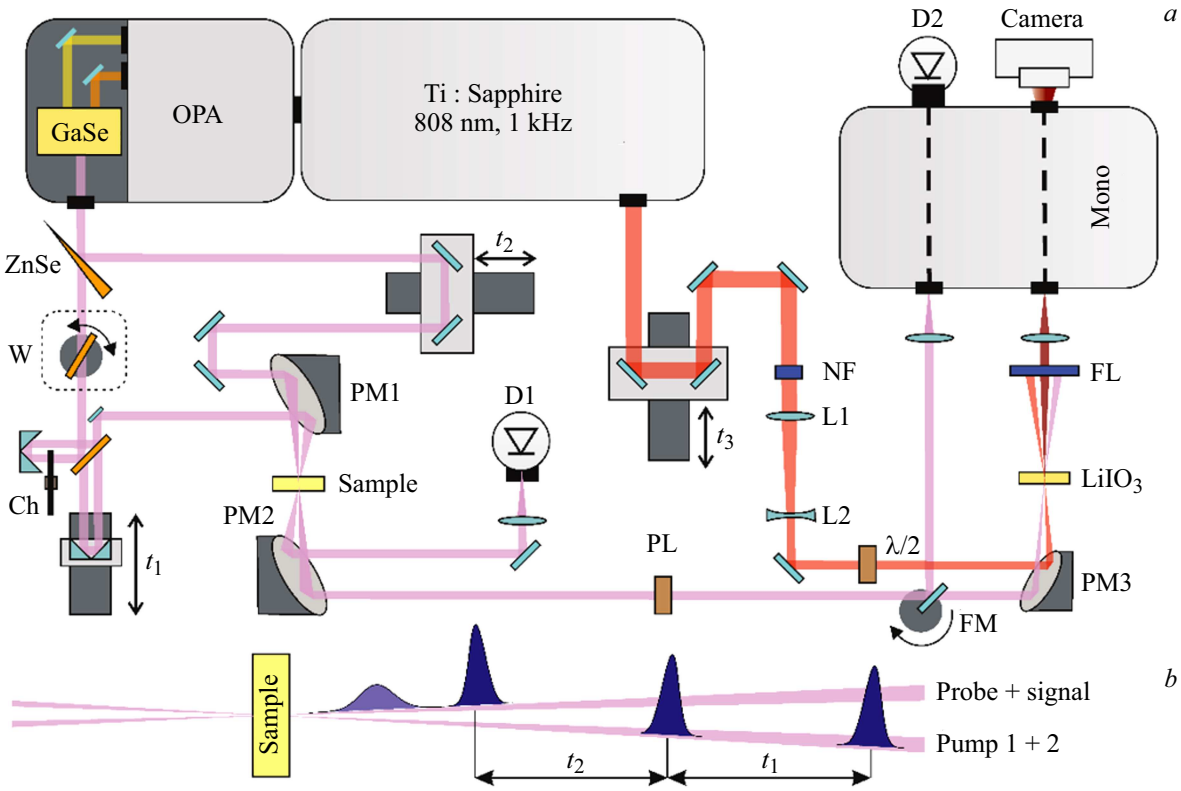

Figure 1. (*a*) Schematic diagram of a two-dimensional IR spectrometer based on Michelson interferometer using a nonlinear optical crystal to transfer the radiation to the visible region of the spectrum. Ch — chopper (optical shutter), W — wobbler, D1, D2 — MCT detectors, NF — narrowband filter, PL — polarizer, FL — high frequency filter, Mono — monochromator, Camera — kilohertz silicon linear matrix, L1-2 — zoom-out telescope, PM1-3 — parabolic mirror, FM — movable mirror. (*b*) Sequence of IR pulses incident on the sample under study: t_1 — delay between pump pulses, t_2 — delay between the second pump pulse and the probe pulse.

reactions in real time. In the process of transferring the spectrum to the visible region in a nonlinear optical crystal, it is also possible to avoid inherent noise of photodiodes that record the radiation in the mid-IR range. The photon of the radiation under study is not absorbed by the substance, but is transformed in the transmission region of the nonlinear optical material on the $\chi^{(2)}$ square nonlinearity. In accordance with Kirchhoff's law of thermal radiation, the absorption of a medium in thermodynamic equilibrium is equal to its emission, which means that a nonlinear medium that is transparent in the mid-IR range and kept at room temperature will not emit additional thermal photons, introducing distortions into the converted radiation under study.

For the conversion of radiation in the spectral range of $3-6\,\mu$m when mixed with a chirped pump pulse of a Ti:Sapphire laser system, MgO:LN and $LiIO_3$ crystals are the most attractive, possessing wide phase matching of the sum frequency generation process in the region of the central wavelength of 4 and $5\,\mu$m, respectively (Fig. 2). This allows, on the one hand, carrying out correlation measurements in a wider spectral range, covering all modes of interest in the molecular system under study, and, on the other hand, the use of longer crystals, compensating for their relatively low radiation resistance, to increase the conversion efficiency. To transform the IR spectrum in the range of $2000-2080\,\text{cm}^{-1}$, in this study we use a $LiIO_3$ crystal with a thickness of $500\,\mu$m, cut out at an angle of $\theta = 21.5^\circ$ and $\varphi = 0^\circ$.

A picosecond pump pulse at a central wavelength of 808 nm is taken from the unused reflection of the uncompressed pulse into the zero order of diffraction grating of the regenerative chirped pulse amplifier compressor. Then, the beam passes through a narrow-band filter (NF in Fig. 1) with a bandwidth of 3 nm to remove spectral components that do not participate in the conversion and, accordingly, reduce the radiation load on the nonlinear crystal. To match the sizes of the waists of the radiation under study and the reference radiation, a compression telescope formed by focusing and scattering lenses (L1 and L2 in Fig. 1) is installed downstream of the narrow-band filter, due to which, at the focus of 150 mm of the off-axis parabolic mirror, the waists of the crossed beams are equal to each other, their diameter is $150\,\mu$m, which makes it possible to achieve high efficiency of the nonlinear optical conversion. The excess energy of the picosecond pulse was attenuated by a set of neutral filters to the maximum peak intensity, at which no optical breakdown of the crystal takes place yet, i.e. about $0.7{\cdot}10^9\,\text{W/cm}^2$. The probe pulse energy at the central wavelength of $5\,\mu$m downstream of the sample was

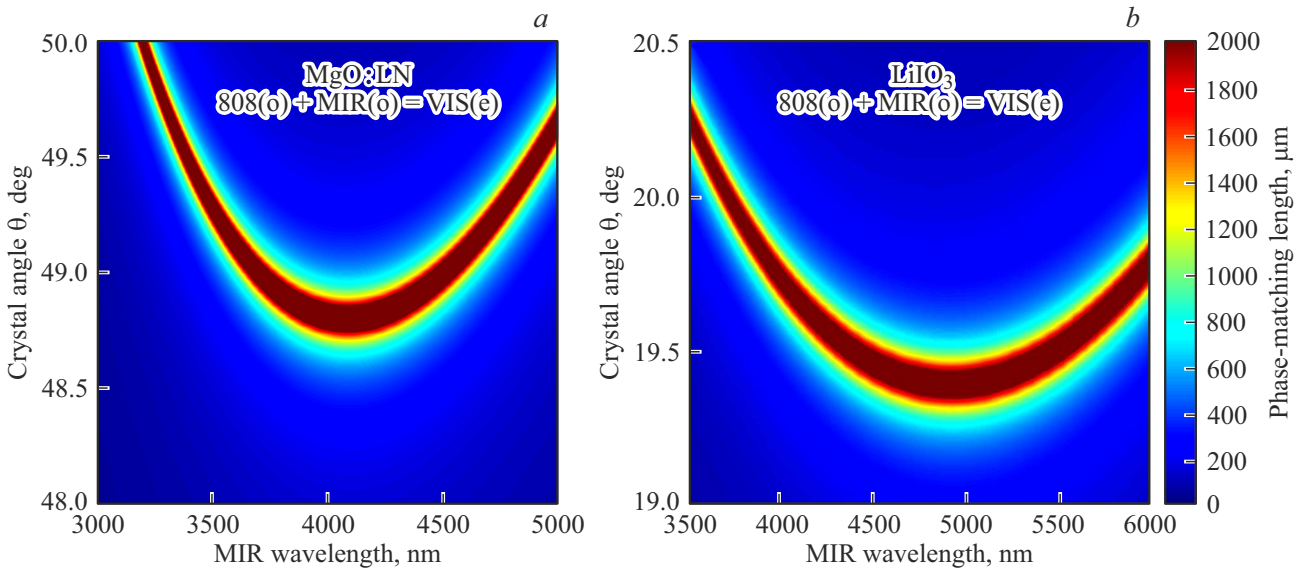

Figure 2. Two-dimensional map of phase-matching lengths of the sum frequency generation process when mixing the radiation in the mid-IR range with a pump pulse at a central wavelength of 808 nm in a MgO:LN crystal (*a*) and a $LiIO_3$ crystal (*b*) depending on the wavelength and crystal orientation.

150 nJ, and the energy of the pulse at the sum frequency (at a wavelength of about 700 nm) was 2.4 nJ. Thus, the conversion efficiency was about 11% in terms of the number of photons.

As a result of up-conversion of IR radiation into the visible region when mixed with a picosecond pulse at a central wavelength of 808 nm, the spectrum of the main absorption lines of the octacarbonyl dicobalt solution in the range of $2000-2080\,cm^{-1}$ is transferred into a spectral region with a width of only 4 nm — from 691.5 to 695.5 nm (Fig. 3, *a*). To record such a narrow spectrum in the visible region with a resolution of at least 100 points, a M522 „SolarLS“ monochromator with a 1200 1/mm grating was used. Instead of an exit slit, a TCN-1209-U „Mightex“ high-speed linear camera was installed behind the monochromator, allowing recording of a 12-bit image with a size of 1×2048 pixels synchronously with an external trigger at a frequency of 1000 frames per second with a minimum exposure time of 0.3 ms. The pixel size of the matrix of this camera is 14 μm, which, in combination with the inverse linear dispersion of the monochromator of 1.4 nm/mm, makes it possible to achieve a spectral resolution of 0.02 nm. To collect data, synchronize and control the laser system, a NI USB-6356 (BNC) general-purpose ADC-DAC module by National Instruments is used, the software is written in the LabVIEW environment and is optimized for multi-core processing of the continuous large data stream from the camera and detectors operating at kilohertz frequency.

As a sample for testing the technique of recording two-dimensional IR spectrum with nonlinear optical frequency conversion, we have chosen the previously used a carbonyl complex of cobalt, $Co_2(CO)_8$ [10]. The spectrum of this compound in a hexane solution has pronounced absorption lines near $2000\,cm^{-1}$ (which corresponds to a wavelength of about 5 μm). In a solution of octacarbonyl cobalt alkanes, it exists in two stable states, corresponding to different isomers [10–12]. The IR spectrum of each isomer contains several CO absorption bands at slightly different frequencies corresponding to different vibrational modes. This results in the emergence of off-diagonal peaks in the two-dimensional spectrum, associated both with the redistribution of energy within one isomer and with a change in the state of the molecule and its transition from one isomer to another after excitation of the vibration by a femtosecond laser pulse. This property makes it possible to use the carbonyl complex of cobalt as a convenient test sample to optimize the procedure for recording and processing nonlinear signal to form a two-dimensional spectrum. The substance under study in a liquid state is placed in a cuvette consisting of two optical windows made of calcium fluoride, between which there is a calibrated fluoroplastic spacer with a thickness of 50 to 1000 μm. The small thickness of the cuvette makes it possible to increase the ratio of the efficiency of the nonlinear process, which occurs only in the focal volume near the waist of the intersecting beams, to linear absorption in the entire exposed volume of the substance. Also, a decrease in the thickness of the cuvette results in expansion of the range of angles where the phase matching conditions are met for a nonlinear signal arising as a result of four-wave interaction. The concentration of the cobalt carbonyl solution in standard hexane was selected in such a way that the absorbance at the wavelength corresponding to the highest absorption in the region of $2000\,cm^{-1}$ was about unity with a thickness of the liquid layer under study of about 100 μm.

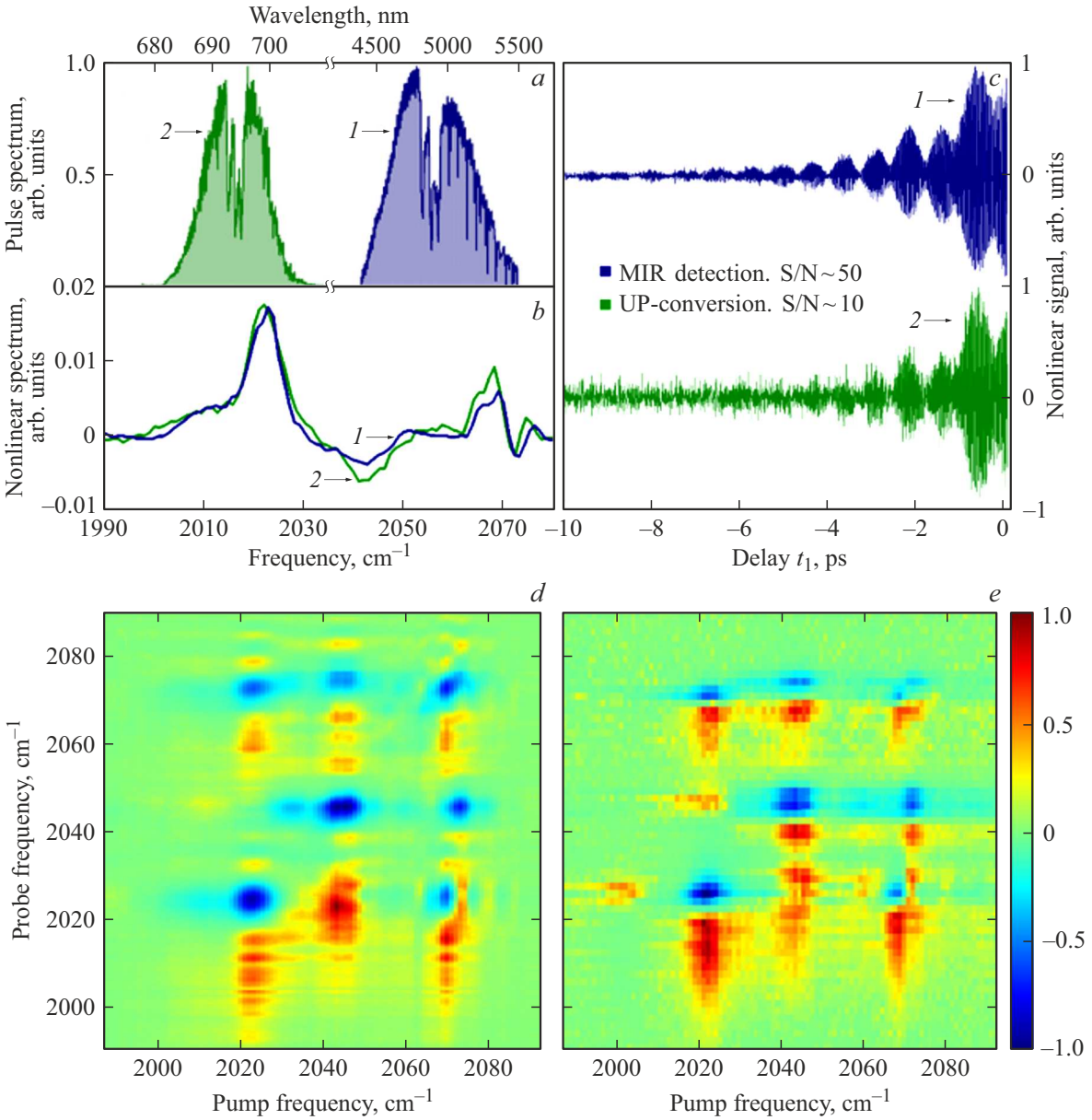

Figure 3. (*a*) The spectrum of the IR pulse downstream of the cuvette with the sample, measured in the IR range (blue curve, *1*) and after up-conversion (green curve, *2*). (*b*) Nonlinear spectrum of octacarbonyl dicobalt at a detection wavelength of 4942 nm and the corresponding signal (*c*), detected by an MCT-diode (blue curves, *1*) and one element of kilohertz silicon linear matrix (green curves, *2*). (*d*) Two-dimensional IR spectrum of octacarbonyl dicobalt measured in a single scan of delay t_1 using the method of up-conversion to the visible spectral region and with direct detection of mid-IR radiation by a liquid nitrogen-cooled MCT-diode (*e*).

Fig. 3, *d*–*e* shows the results of measuring the two-dimensional IR absorption spectrum of octacarbonyl dicobalt by two different methods: using direct detection of radiation with a MCT-diode cooled with liquid nitrogen (Fig. 3 , *d*), as well as by the method of nonlinear optical frequency conversion to the visible frequency range (Fig. 3, *e*). Due to the use of a multichannel linear matrix, the latter method provides a significant gain in the measurement speed, but loses on signal-to-noise ratio to the IR diode cooled to cryotemperatures. Fig. 3, *c* shows the normalized dependence of nonlinear signal of the diode at a fixed wavelength of $\lambda = 4942$ nm on the delay t_1 and the corresponding dependence of the signal of one camera pixel after frequency conversion. The calculated ratio of root-mean-square signal to root-mean-square noise at a large delay for one pixel turns out to be approximately 5 times lower, however, in the overall picture this disadvantage is compensated by the high density of camera pixels, which exceeds the actual optical resolution of the method.

The use of a special window function when processing a nonlinear signal with a sufficiently high signal-to-noise ratio makes it possible to significantly increase the spectral

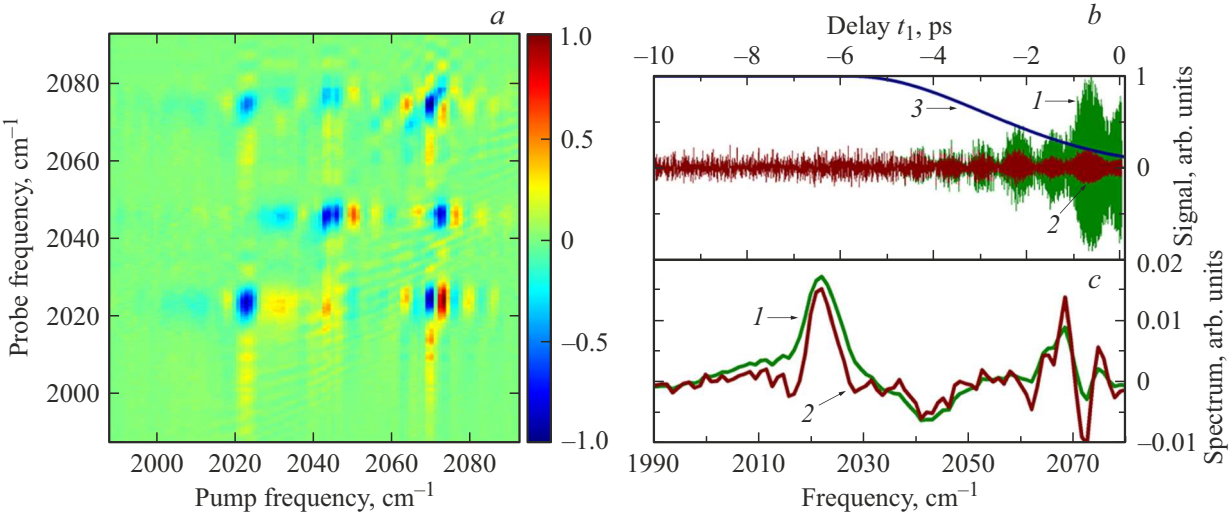

Figure 4. (*a*) Two-dimensional IR spectrum of octacarbonyl dicobalt calculated using a window function. (*b*) Nonlinear signal at a wavelength of 4942 nm before (green curve, *1*) and after (brown curve, *2*) application of the exponential window function (blue curve, *3*). (*c*) Spectrum calculated from the signal with the use of a window function (brown curve, *2*) and without it (green curve, *1*).

resolution of the method along the pump axis. The window function is selected in such a way as to compensate for the signal attenuation with increasing delay (in this case, a $\exp(-t/a - (t - t_{\max})^2/b)$ exponential function was used (blue curve in Fig. 4). However, when implementing this approach, the signal-to-noise ratio decreases significantly — for the signal shown in Fig. 4, this ratio decreased by 10 times to a value of the order of 1. Therefore, when building up a two-dimensional spectrum, the results of 10 measurements were averaged, which took no more than 2 min. As a result of applying window filtering of the signal, it was possible to resolve nearby vibrational lines of octacarbonyl dicobalt at frequencies of 2044 cm and 2049 cm^{-1} along the pump axis (Fig. 4, *a*).

At the same time, it was not possible to resolve these individual oscillations along the detection axis, because the resolution along two axes on a two-dimensional graph is determined by fundamentally different elements of the set-up: the resolution of the pump spectrum (Fourier transform) depends on the effective delay scanning range t_1, where the fading nonlinear signal is still distinguishable against the background noise, and the resolution along the detection axis is determined by the characteristics of the spectral device (monochromator and linear camera) and the spectral width of the reference radiation involved in the process of up-conversion. Thus, the use of a broadband chirped pulse as a reference leads to the situation that as a result of its addition to the nonlinear signal under study, spectral broadening of the lines takes place: a slowly fading IR signal (with a duration of more than 10 ps) interacts with various spectral components of the chirped pump pulse, separated by time. This disadvantage of the technique can be overcome at the stage of data processing by the method of deconvolution of the measured spectrum, taking into account the known phase modulation of the reference pulse [13].

An alternative approach is to implement a nonlinear optical conversion with a dispersed beam of IR radiation, in which the spectral resolution is determined by the properties of the spectral device in the mid-IR range and does not depend on the spectral bandwidth of the reference pulse[14].

In the process of two-dimensional spectrum recording, the detector receives not only the radiation of the probe pulse and the nonlinear response of the substance under study, but also the pump pulses, which are partially scattered on inhomogeneities of the sample and the surface of the cuvette and propagate in the same direction as the probe pulse. Taking into account the fact that pump pulses, as a rule, have an order of magnitude greater intensity, the interference of even a small fraction of them with the probe pulse leads to a significant background illumination, which in two-dimensional spectra appears as a band along the diagonal of the image. If only off-diagonal peaks of the two-dimensional spectrum are of interest for the study, then this illumination can be ignored, otherwise it is necessary to use additional methods to determine and subtract it. The detected signal, accurate to the first order of smallness, consists of four main terms:

$$S \propto E^2_{\text{probe}} + E_{\text{probe}}E_{\text{NL}} + E_{\text{probe}}E_{\text{pump1}} + E_{\text{probe}}E_{\text{pump2}},$$

where E^2_{probe} and $E_{\text{probe}}E_{\text{pump2}}$ disappear after the Fourier transform over the delay t_1, because they do not depend on it, $E_{\text{probe}}E_{\text{NL}}$ is useful signal, and $E_{\text{probe}}E_{\text{pump1}}$ is background illumination that must be removed from the spectrum. In the simplest case, a mechanical chopper is used for this (Ch in Fig. 1, *a*), installed in the stationary arm of the pump interferometer, tuned to half the pulse repetition rate, and blocking every second pulse. In this case, all odd sampling

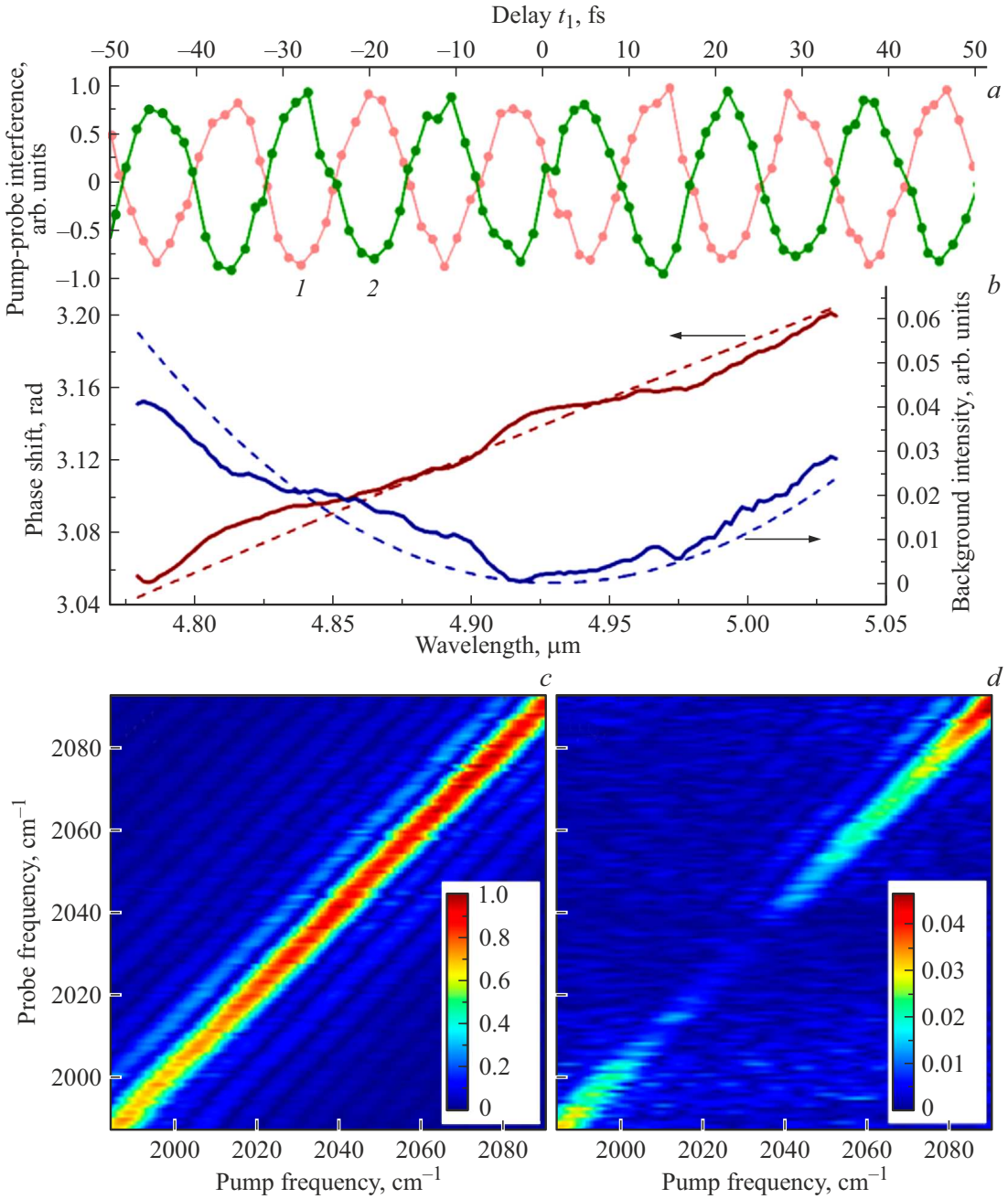

Figure 5. (*a*) The interference of the probe pulse and the moving pump pulse recorded behind the monochromator at a wavelength of 4930 nm with optimal adjustment of the wobbler oscillation amplitude. Odd (pink curve, *1*) and even (green curve, *2*) sampling points corresponding to different wobbler angles are shown separately. (*b*) Relative phase shift of the interference between even and odd sampling points depending on the wavelength (solid brown curve — experimental data, dashed brown curve — calculation, caption on the left) and its corresponding residual intensity background illumination (solid blue curve — experimental data, dashed blue curve — calculation, caption on the right). (*c, d*) Measured two-dimensional spectrum of an empty cuvette with the wobbler turned off (*c*) and with the wobbler turned on (*d*), the oscillation amplitude of which is optimized for a wavelength of 4930 nm ($\approx 2028\,\text{cm}^{-1}$).

points will contain information about the useful signal with illumination, and even ones will contain only illumination. Subtraction of spectra calculated independently from two halves of the sample makes it possible to remove illumination, while halving the number of points with a useful signal, which is the main disadvantage of the chopper leading to the doubling of the registration time of a two-dimensional spectrum.

As an alternative to the optical chopper, to eliminate the background illumination, a device can be used that reverses the phase of every second pump pulse (often in the English literature it is called a „wobbler“ (W in Fig. 1, *A*). The

operating principle of such a device is based on introducing an additional optical delay into the pump beam, varying with a frequency half the pulse repetition rate [15]. This device in our experiments was made in an original design using a non-resonant galvanic scanner from a laser projector and a plane-parallel zinc selenide plate with a size of 9−18 mm and a thickness of 1 mm, glued instead of mirror onto the galvanic scanning head. The plate is installed at the Brewster angle to the pump radiation in front of the Michelson interferometer, the rotation of the scanner is controlled by an analog signal in the form of a sine wave with a frequency of 500 Hz, generated synchronously with pulse repetition rate by the NI USB-6356 (BNC) input-output device National Instruments. The phase of the control sine signal is selected in such a way that two successive pump pulses pass through the plate at the moments of time when it deviates by a maximum angle from the equilibrium position in one and the other direction, respectively. In this case, the amplitude of the plate oscillations determines the delay of even and odd pulses relative to each other. This method makes it possible to accurately reverse the phase of pulses at one specific wavelength, as a result of which the interference spectrum of the probe pulse with the moving pump pulse is effectively zeroed when calculated over the entire scanning range. At the same time, the third order nonlinear response phase

$$\varphi_{\mathrm{NL}} = \mp\varphi_{\mathrm{pump1}} \pm \varphi_{\mathrm{pump2}} + \varphi_{\mathrm{probe}}$$

remains unchanged for even and odd pulses, because it depends on the phase difference between the two pump pulses, which makes it possible to obtain twice as much useful signal at the same scanning speed compared to the optical chopper. However, the dispersion of zinc selenide results in the situation that with increasing distance from the wavelength for which the vibration amplitude of the plate is optimized, the value of the phase difference deviates from π, which leads to incomplete suppression of the interference spectrum (Fig. 5, *c, d*). In the presented experiments, the amplitude of the wobbler oscillations was chosen in such a way as to accurately suppress the interference at a wavelength of 4930 nm (Fig. 5, *a*). Fig. 5, *b* shows the experimentally obtained dependences of the relative phase shift and the intensity of parasitic interference on wavelength, as well as the corresponding theoretical dependences calculated for millimeter-plate of zinc selenide.

It can be seen from the presented results that the use of the wobbler based on a plane-parallel zinc selenide plate makes it possible to completely suppress the background illumination caused by the interference of the probe pulse with the moving pump pulse only at one specific wavelength (in this experiment, a wavelength of 4930 nm was chosen). Around it, in the spectral range with a width of 100 cm^{-1}, the signal/background ratio increases by more than 20 times, and in the spectral range with a width of 20 cm^{-1} it increases by more than 100 times compared to measurements without a wobbler and an optical chopper. When directly detecting a nonlinear signal in the mid-IR range with a single-element detector, the use of a wobbler to suppress background illumination is more preferable than an optical chopper, because the amplitude of plate oscillations can be adjusted automatically in the process of scanning the wavelength with a monochromator, ensuring complete suppression of the unwanted interference throughout the entire range of wavelengths under study and giving a 2-fold gain in scanning speed due to a larger number of „useful" points. When using the up-conversion technique to simultaneously record a nonlinear response in a wide range of wavelengths using a wobbler, it is necessary to take into account the incomplete compensation of background illumination, which is manifested at the edges of the spectrum due to the dispersion of the zinc selenide plate (Fig. 5, *b*).

For the theoretical modeling of the obtained two-dimensional IR spectrum, a quantum description of the process of pump fields interaction with the medium under study is used using the formalism of the density matrix operator and analysis of its evolution (and, accordingly, analysis of the dynamic response of the substance) based on solving the Bloch-Redfield equation. To model the response function of the medium in the scheme of two-dimensional IR Fourier spectroscopy, it is necessary to find the Hamiltonian of the system under study [16,17]. The complete Hamiltonian is given by the sum of the eigen Hamiltonian of the system $\hat{H}_0$ and the interaction operator $\hat{V}(t)$ in the dipole approximation with an external „classical" field. All significant vibrational modes can be represented as three-level anharmonic oscillators (the three-level approximation and anharmonicity quadratic in the number of bosons are sufficient for modeling the two-dimensional spectrum [18]). The full Hamiltonian can be rewritten in the approximation of local modes coupled by energy transfer interactions; this also allows the use of a number of approximate calculation methods [19]. General form of the Hamiltonian is as follows:

$$\begin{aligned}\hat{H}(t) = &\sum_n^N \hbar\omega_n(t)\hat{a}_n^\dagger\hat{a}_n - \frac{1}{2}\sum_n^N K_n(t)\hat{a}_n^\dagger\hat{a}_n\hat{a}_n^\dagger\hat{a}_n + \\ &+ \sum\nolimits_{n\neq m}^N J_{nm}(t)\hat{a}_n^\dagger\hat{a}_m + \sum\nolimits_{nmkl}^N J_{nmkl}(t)\hat{a}_n^\dagger\hat{a}_m\hat{a}_k^\dagger\hat{a}_l + \\ &+ \sum\nolimits_n^N \vec{E}(t)\vec{\mu}_n(t)(\hat{a}_n^\dagger + \hat{a}_n),\end{aligned} \tag{5}$$

where the first four terms are responsible for the energies of normal vibrations in the molecule and intramolecular interactions ($\hat{H}_0$), and the last one is responsible for the coupling with the external field in ($\hat{V}(t)$).

The modeling of the nonlinear signal resulting from the interaction between the quantum system and the pump fields is described through the density matrix formalism. Assuming that the change in the Hamiltonian of the system caused by the external field is small, perturbation theory with expansion in a small correction $\hat{V}(t)$ is used to find

the evolution of the system. In the perturbation theory, the density matrix is represented as the following expansion:

$$\hat{\rho}(t) \approx \hat{\rho}^0(t) + \hat{\rho}^1(t) + \hat{\rho}^2(t) + \hat{\rho}^3(t) + \cdots .$$

The zero term is the exact solution to the problem in the absence of perturbation. Then the evolution of corrections to the state is represented by the following equation:

$$\frac{d|\rho^{(n)}(t)\rangle\rangle}{dt} = \frac{1}{i\hbar}\hat{\hat{L}}_0(t)|\rho^{(n)}(t)\rangle\rangle + \frac{1}{i\hbar}\hat{\hat{L}}_{int}(t)|\rho^{(n-1)}(t)\rangle\rangle, \quad (6)$$

where $\hat{\hat{L}}_0$ is Liouville superoperator for $\hat{H}_0$, $\hat{\hat{L}}_{int}$ is Liouville superoperator for $\hat{V}(t)$. Before the start of interaction, all fields are absent, which determines the boundary condition of $|\rho^{(n)}(-\infty)\rangle\rangle = 0$ for all terms of the expansion except the zero term. In this case, the solution can be written in the following form:

$$|\rho^{(n)}(t)\rangle\rangle = -\frac{i}{\hbar}\int_{-\infty}^{t} d\tau \hat{\hat{G}}(t-\tau)\hat{\hat{L}}_{int}(\tau)|\rho^{(n-1)}(\tau)\rangle\rangle. \quad (7)$$

Taking light pulses to be infinitely short, solution (7) can be simplified as follows:

$$|\rho^{(n)}(t)\rangle\rangle = -\frac{i}{\hbar}\hat{\hat{G}}(t-t_n)\hat{\hat{\mu}}(t_n)|\rho^{(n-1)}(t_n)\rangle\rangle.$$

The above Hamiltonian (5) allows specifying all states of a quantum closed system that can be reproduced in the nonlinear response, however, it does not in any way determine the interaction with the external environment, dissipative processes and processes of intermode interaction involving degrees of freedom of the reservoir. To describe dissipative systems, there is the Bloch-Redfield equation for the evolution of the density matrix in the form of an equation with a time-independent superoperator, which includes population relaxation and cross-relaxation, coherence relaxation, coherence transfer [20,21]. In this approximation, the external environment („the reservoir“) and the quantum system can be determined independently. The coupling of the system with the reservoir is specified by operators defined in the Hilbert space of the system and its state at previous moments of time. To approximate Markov dynamics, it is necessary to take into account that the times of relaxation processes in the reservoir are much shorter than the typical evolution times of the system and the noise correlation function decays in a time shorter than the characteristic evolution time of the system. Then the Bloch-Redfield equation, which derivation is presented [21–23], takes on the following form:

$$\frac{d\hat{\rho}(t)}{dt} = \frac{1}{i\hbar}\left[\hat{H}_S, \hat{\rho}\right] - \frac{1}{\hbar^2}\sum\nolimits_{i,k}(\hat{S}_j\hat{D}_{jk}\hat{\rho}(t) - \hat{D}_{jk}\hat{\rho}(t)\hat{S}_j + \\ + \hat{\rho}(t)\hat{D'}_{jk}\hat{S}_j - \hat{S}_j\hat{\rho}(t)\hat{D'_j}k). \quad (8)$$

The entire second term can be called the relaxation superoperator R, and then the equation takes on a more compact form:

$$i\hbar\frac{d\hat{\rho}(t)}{dt} = [\hat{H}(t), \hat{\rho}(t)] + i\hbar\hat{\hat{R}}\hat{\rho}(t). \quad (9)$$

The Bloch-Redfield equation written in this form was used in our theoretical modeling. Due to the fact that the pump and probe pulses have different directions, the equations to be solved must take into account the geometry of the experiment. This is achieved by substituting into the evolution only those complex components of the light field, the interaction with which will lead to the emission of a signal in the direction to be detected. In the general case, there can be two directions of interest in a two-dimensional spectroscopy experiment: rephasing and non-rephasing. The names of the directions indicate the presence or absence of a photon echo effect from an ensemble of oscillators. This effect is due to the fact that in the case of rephasing interaction, the frequencies of the complex components of the first and third pulses have different signs. In this case, the phases of individual particles of an inhomogeneously broadened ensemble, accumulated during the coherence time t_1, effectively acquire the opposite direction of evolution, which leads to the emergence of an optical signal from the ensemble at the time $t_3 = t_1$ relative to the third impulse.

In the case of a non-rephasing interaction, the direction of evolution of the phases of the ensemble particles remains unchanged, which means that the rephasing effect does not occur and the photon echo is not observed. Solving a system of three equations of form (9) yields the evolution of the density matrix operator for the system under study, which makes it possible to find the nonlinear response function. The program code is implemented in Python, within which the evolution of a quantum system with a Hamiltonian of form (5) is calculated by solving equation (9) using the matrix exponential method, after which the third-order nonlinear response function is calculated. The problem was solved within the framework of the secular approximation, i.e. with a time-independent relaxation superoperator; to build up the initial Hamiltonian of a system of form (5), the states were taken into account, where no more than three excitation quanta are involved. The main mode frequencies, as well as their anharmonicity for octacarbonyl dicobalt, obtained in [10,12], were used as the initial data for the calculation. As a result of the calculation, a nonlinear response function of the 3-rd order was obtained and the spectra of its rephasing and non-rephasing parts were calculated (Fig. 6, *a, b*), and a two-dimensional spectrum of the full (sum) response function was built-up, coinciding with good accuracy with the absorption spectrum obtained during the experiment in the „pump-probe“ geometry of beams (Fig. 6, *c*). A comparison of experimental results and numerical modeling shows good qualitative agreement, which suggests the effectiveness of the model and numerical code used and, accordingly, the possibility of using them for the analysis of other molecular systems.

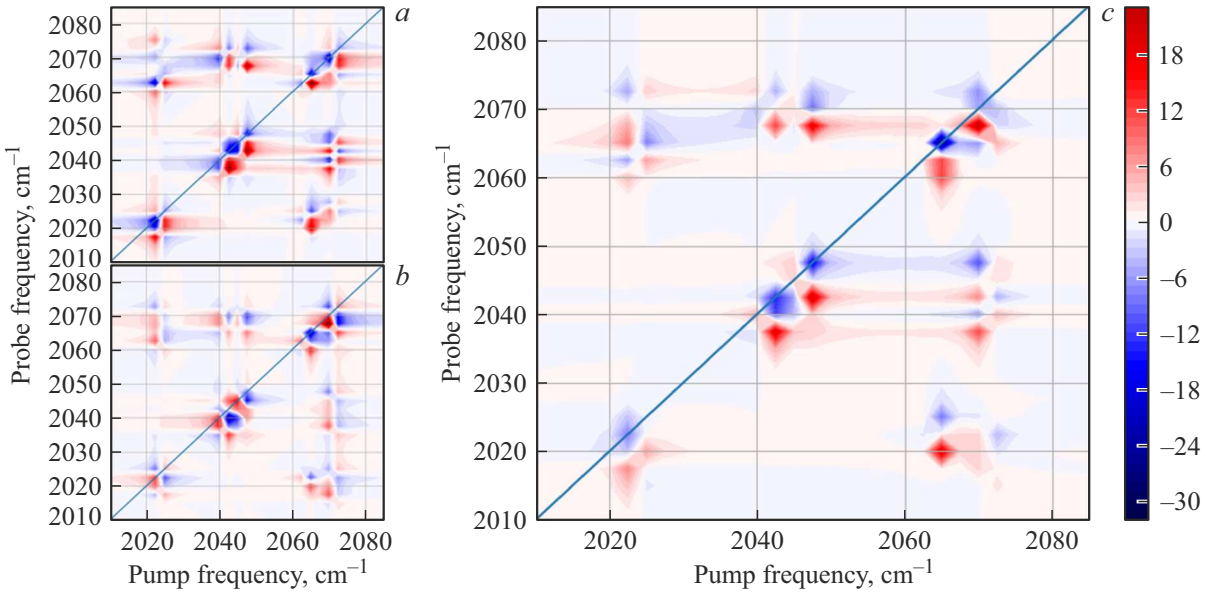

Figure 6. Two-dimensional IR spectrum of octacarbonyl dicobalt, calculated from the rephasing (*a*) and non-rephasing (*b*) parts of the model nonlinear response function, as well as the absorption spectrum (*c*), corresponding to the experimental measurement in the „pump-probe“ beam geometry.

Thus, the study demonstrates that converting radiation into the visible region of the spectrum makes it possible to get rid of the direct measurement of signal in the mid-IR range with expensive detectors that require the use of cryogenic technologies, and to use instead the technologically advanced and affordable multi-channel silicon linear matrices that have high sensitivity and allow one laser shot („single-shot“) registering the radiation spectrum in a wide range.

The demonstrated decrease in the time of measurement of one two-dimensional spectrum by two orders of magnitude makes it possible to observe the fast temporal dynamics of complex molecular compounds. The use of a phase compensation scheme for background illumination makes it possible to suppress the noise arising from parasitic scattering by almost two orders of magnitude and double the measurement speed for both modalities of the recording system. Numerical modeling of the process of interaction of pump fields with the medium under study using the formalism of the density matrix operator and analysis of its evolution based on the solution to the Bloch-Redfield equation made it possible to qualitatively reproduce the features of the two-dimensional IR absorption spectrum of octacarbonyl dicobalt and make a conclusion about the applicability of the code used for analyzing the dynamics of molecular vibrations of a wide range of substances.

Acknowledgments

The authors would like to thank Professor A.M. Zheltikov, the head of the scientific group, for his comprehensive support of the work.

Funding

The study was carried out with funding from the Russian Science Foundation: grant 22-12-00149 regarding the development of a technique for nonlinear optical signal recording and grant 22-72-10044 regarding the numerical modeling of two-dimensional spectra.

Conflict of interest

The authors declare that they have no conflict of interest.

References

[1] S. Mukamel. *Principles of Nonlinear Optical Spectroscopy* (Oxford University Press, NY., 1995).
[2] M.C. Asplund, M.T. Zanni, R.M. Hochstrasser. PNAS, **97** (15), 8219–8224 (2000). DOI: 10.1073/pnas.140227997
[3] P. Hamm, M. Lim, R.M. Hochstrasser. J. Phys. Chem. B, **102** (31), 6123?6138 (1998). DOI: 10.1021/jp9813286
[4] S. Mukamel, Y. Tanimura, P. Hamm. Acc. Chem. Res., **42** (9), 1207–1209 (2009). DOI: 10.1021/ar900227m
[5] P. Hamm, M. Zanni. *Concepts and Methods of 2D Infrared Spectroscopy* (Cambridge University Press, 2011). DOI: 10.1017/CBO9780511675935
[6] S.T. Cundiff, S. Mukamel. Phys. Today, **66**, 44–49 (2013). DOI: 10.1063/PT.3.2047
[7] A.L. Le Sueur, R.E. Hornessa, M.C. Thielges. Analyst, **140**, 4336–4349 (2015). DOI: 10.1039/C5AN00558B
[8] J. Helbing, P. Hamm. J. Opt. Soc. Am. B, **28** (1), 171–178 (2011). DOI: 10.1364/JOSAB.28.000171
[9] E.A. Stepanov, A.A. Lanin, A.A. Voronin, A.B. Fedotov, A.M. Zheltikov. Phys. Rev. Lett., **117** (4), 043901 (2016). DOI: 10.1103/PhysRevLett.117.043901

[10] E.A. Stepanov, A.N. Zhdanov, I.V. Savitsky, P.B. Glek, A.A. Lanin, A.B. Fedotov, A.M. Zheltikov, Kvant. elektron., **52** (3), 227–232 (2022) (in Russian). DOI: 10.1070/QEL18004
[11] R.L. Sweany, T.L. Brown. Inorg. Chem., **16** (2), 415?421 (1977). DOI: 10.1021/ic50168a037
[12] J.M. Anna, K.J. Kubarych. Chem. Phys., **133**, 174506 (2010). DOI: 10.1063/1.3492724
[13] J.M. Anna, M.J. Nee, C.R. Baiz, R. McCanne, K.J. Kubarych. J. Opt. Soc. Am. B, **27**, 382–393 (2010). DOI: 10.1364/JOSAB.27.000382
[14] M.F. DeCamp, L.P. DeFlores, K.C. Jones, A. Tokmakoff. Opt. Express, **15** (1), 233–241 (2007). DOI: 10.1364/OE.15.000233
[15] R. Bloem, S. Garrett-Roe, H. Strzalka, P. Hamm, P. Donaldson. Opt. Express, **18** (26), 27067–27078 (2010). DOI: 10.1364/OE.18.027067
[16] V. May, O. Kuhn. *Charge and Energy Transfer Dynamics in Molecular Systems* (Wiley-VCH Verlag GmbH & Co. KGaA, 2011). DOI: 10.1002/9783527633791
[17] M.P. Mueller. *Fundamentals of Quantum Chemistry: Molecular Spectroscopy and Modern Electronic Structure* Computations (Springer New York, NY., 2007). DOI: 10.1007/b113924
[18] T. Jansen, S. Saito, J. Jeon, M. Cho. J. Chem. Phys., **150** (10), 100901 (2019). DOI: 10.1063/1.5083966
[19] C.R. Baiz, K.J. Kubarych, E. Geva, E.L. Sibert. J. Phys. Chem. A, **115** (21), 5354–5363 (2011). DOI: 10.1021/jp201641h
[20] G. Lindblad. Commun. Math. Phys., **48** (2), 119?130 (1976). DOI: 10.1007/BF01608499
[21] D. Manzano. AIP Advances, **10** (2), 025106 (2020). DOI: 10.1063/1.5115323
[22] J. Jeske, J.H. Cole. Phys. Rev. A, **87**, 052138 (2013). DOI: 10.1103/PhysRevA.87.052138
[23] J. Jeske, David J. Ing, M.B. Plenio, S.F. Huelga, J.H. Cole. J. Chem. Phys., **142** (6), 064104 (2015). DOI: 10.1063/1.4907370

Translated by Y.Alekseev